

1 Introduction

Reason for measuring in reflection with open, short or matched termination: Effective length is lower, avoiding spurious resonances (Paris)? Case of open termination: can apply bias voltage.

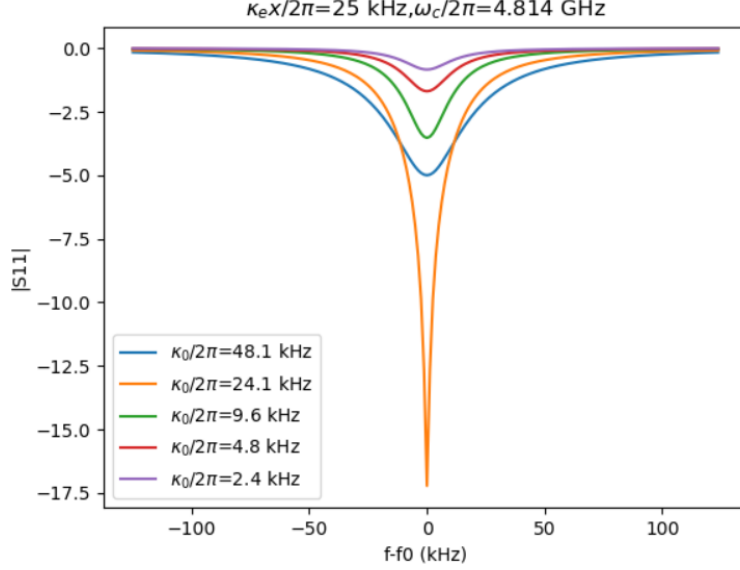
We measured two devices of the type described in [1, 2] on a single chip. We first made measurements in a transmission configuration at 12 mK and at 215 mK. The model of [3] was fitted to S21 measurements of the cavities. The best fit values of the internal damping had a pump power dependence consistent with saturation of TLS, in agreement with the observations of [4, 5]. The thermomechanical noise of one device was also measured at 215 mK, at which temperature we believe the mechanical mode is in thermal equilibrium with the cryostat. The pump frequency was close to the resonance frequency of the microwave cavity (“green” pumping). We then used the damping of the cavity obtained from our S21 fits along with an expression for the microwave output spectrum obtained from input/output theory [6] to extract the phonon population of the mechanical mode. We found that this population was independent of pump power, as expected for green pumping.

We also made measurements with open or short terminations of the microwave feedline at one end of the sample holder (see ‘cavity power dependence.pptx’). We found that the dependence of lineshape on pump power depended on the device for a given termination. The relevant circuit model is uncertain because in these samples the termination is separated from the devices by a distance comparable to the microwave wavelength. That would also be the case for a reflection measurement with matched (i.e. 50 Ohms) termination. In other samples with on-chip termination this issue may be avoided due to the smaller separations.

Palacios-Laloy derived (Eq. 2.16 of his thesis)

$$S_{11} = \frac{\kappa_{ex} - \kappa_{in} + 2i\Delta\omega}{\kappa_{ex} + \kappa_{in} - 2i\Delta\omega}.$$

Its magnitude is the same as that of Eq. S74 of [7]. According to this expression, S_{11} can have a non-monotonic dependence on κ_{in} (see ‘EPFL cavity cct model.ipynb’ and the figure below). The sharpening of S11 with internal damping agrees qualitatively with what we sometimes observed with mis-matched termination.



On p. 87 of the green notebook, I wrote a classical circuit model for the case of mismatched termination. I solved it exactly for the case of a transmission line terminated by a superconducting inductor (the primary inductor), which is coupled inductively to a microwave cavity modeled by the secondary inductor, a capacitor and a resistor, all in series. I found

$$S_{11} = \frac{(\omega L_p/Z_0)g - 1}{(\omega L_p/Z_0)g + 1}$$

where

$$g = i + \frac{\kappa_{ex}}{\kappa_{in} + 2i(\omega - \omega_c)}$$

$$\kappa_{ex} \equiv \frac{\omega_c M^2}{L_p L_s}$$

$$\kappa_{in} \equiv \frac{R}{L_s}$$

The κ parameters I defined might not correspond to the ones that appear in our expression for the optomechanical output spectrum. My model has three parameters related to the primary inductance L_p , the mutual inductance and the resistance. It is possible to reduce my model to the simpler one derived by Palacios-Laloy from input/output theory, which has only two parameters?

Chegnizadeh *et al.* measured a hybridized anti-symmetric resonance of microwave device in reflection and observed the resonance become shallower with stored photon number (Fig. S17 of [7]). They fitted an expression for S_{11} (Eq.

S77) in which a Kerr term was added to Eq. S74 to their measurements and found that the internal damping decreased with stored photon number over part of the measurement range. This part of the range seems to coincide with the range where the resonance becomes shallower with photon number.

2 Experiment

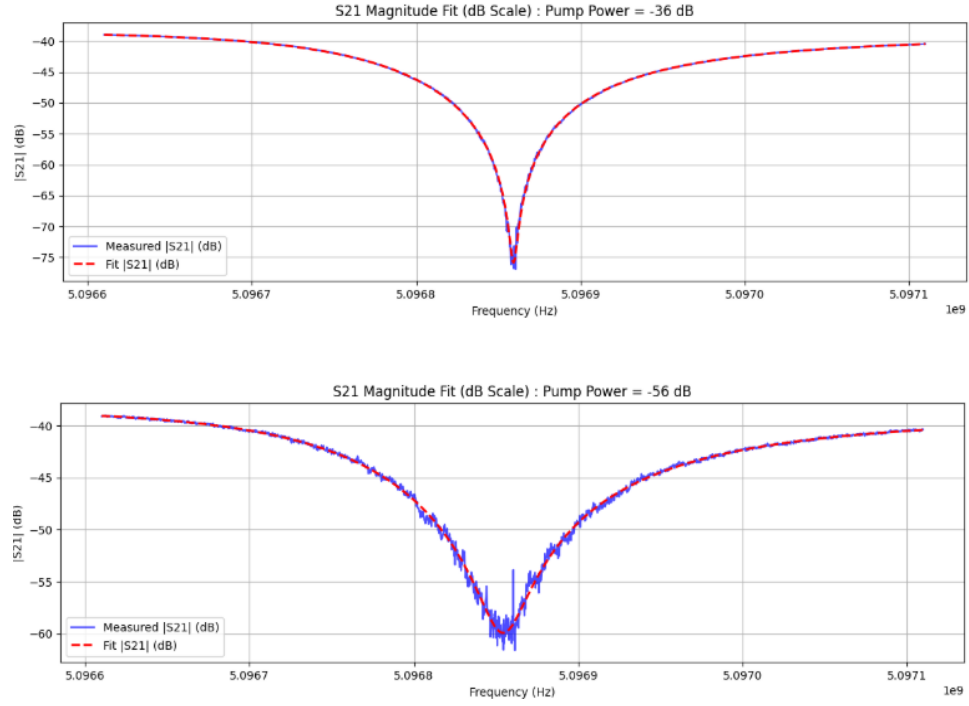
The chip contains devices distributed along a central microwave feedline as described in [1, 2]. However, optical images of these devices seem to show curvature of the drums at room temperature. See photos in 'EPFL collab/sample1' folder. The identifier on the chip is 'Ch_6B-41 20210222'.

For the measurements in transmission, the sample was clamped to the mixing chamber plate of the Bluefors (BF1). See 'microwave circuit.pptx' in this paper draft folder. Initial cavity sweeps were made without the opposition line. The room temperature attenuations were sometimes varied. With the attenuations shown in 'microwave circuit.pptx', we measured -59 dB between VNA input and output at 5.1 GHz (far from cavity resonance). The temperature was measured using a Magnicon noise thermometer (MFFT-1 S/N S0388) screwed directly to the MXC plate. It was connected to channel 2 (yellow) of the Magnicon electronics. In measurements of S21, we set the pump to the frequency of minimum probe transmission. Since the cavity resonance frequency shifted at high pump powers, tuning the pump frequency was sometimes an iterative process. Once the pump frequency was set, the opposition line could be tuned to minimize the transmitted power at the pump frequency.

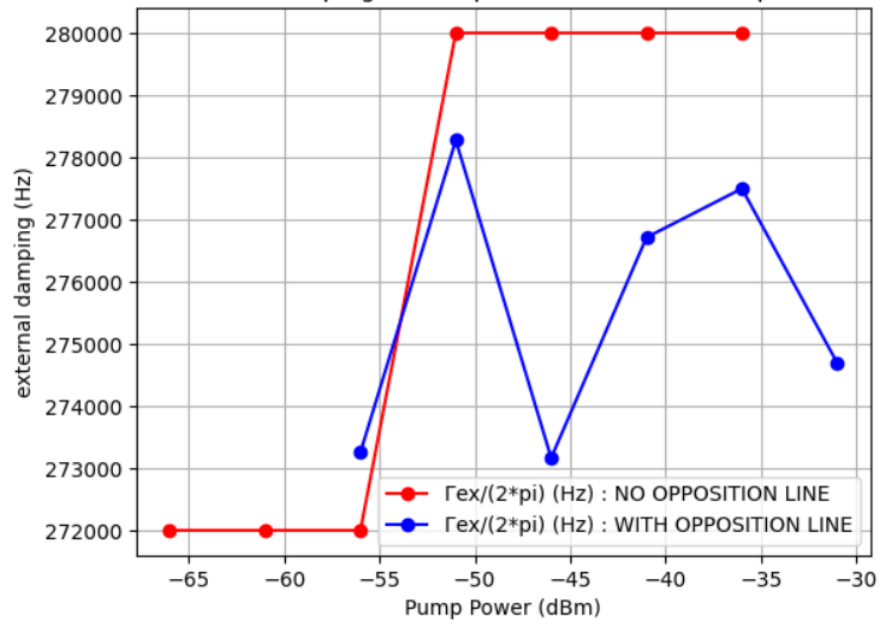
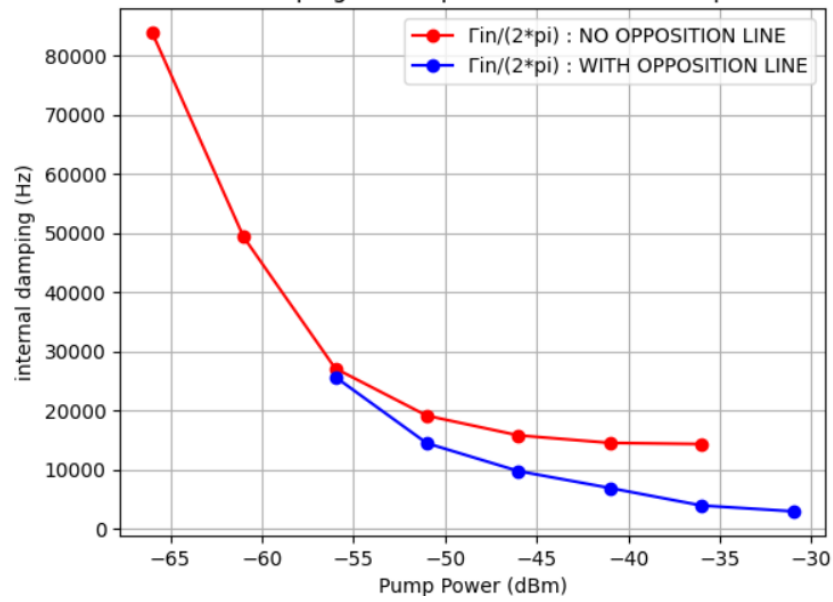
3 Results

3.1 Microwave cavity

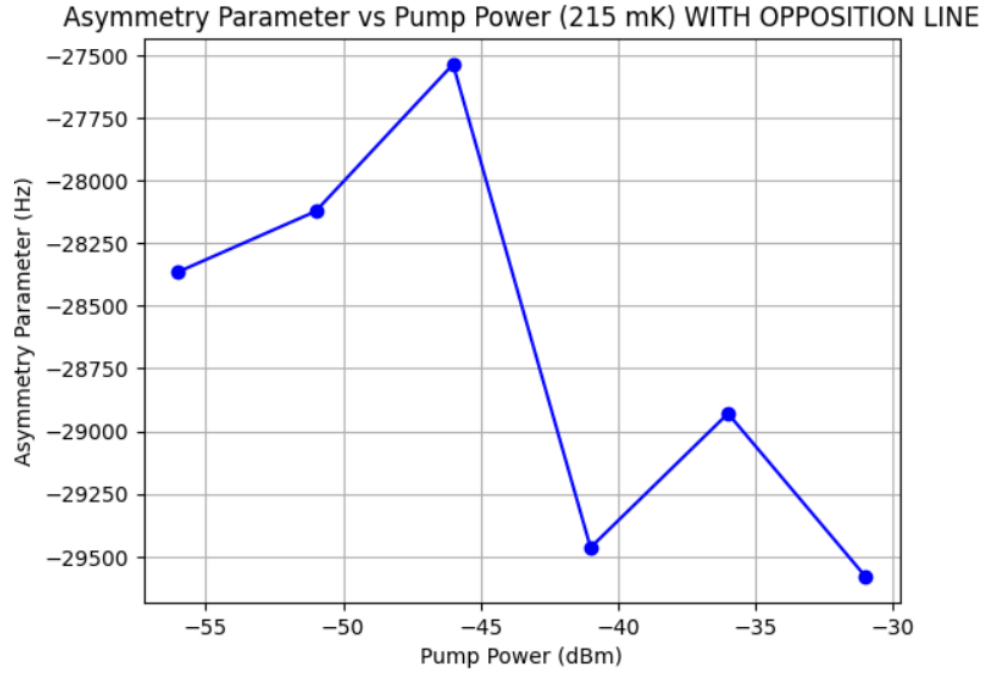
The measurements were analyzed in 'sample 1 S21 and thermomechanics in transmission May 2025(UPDATED).ipynb', where many plots in addition to those shown below can be found. Here are examples of our fits of the expression of [3] to the measured S21 in linear units at 215 mK with the opposition line optimized.



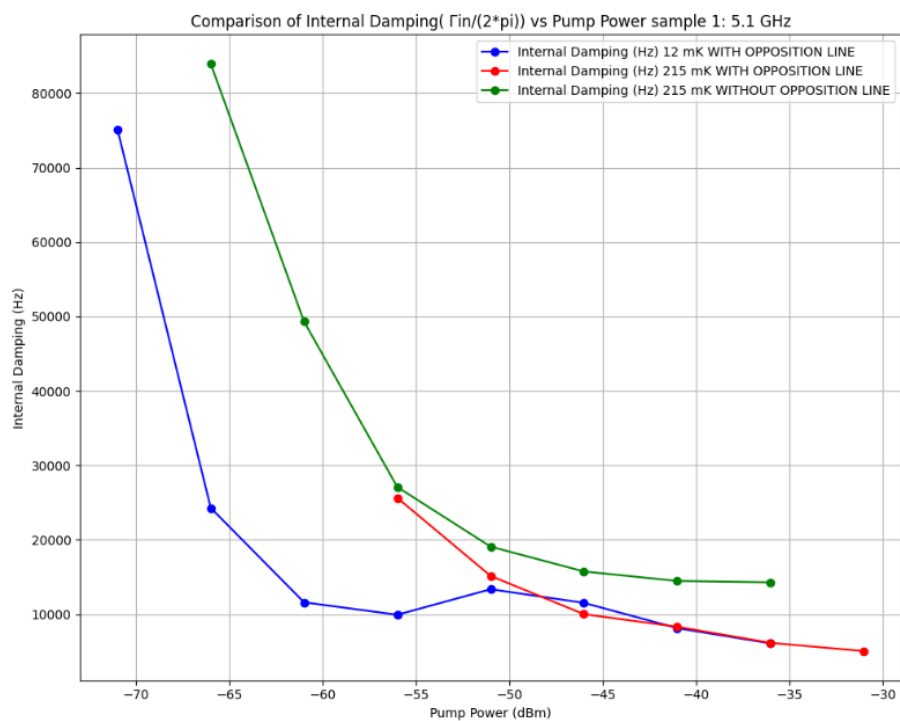
And here is the pump power dependence of the damping measured at 215 mK for the 5.1 GHz device. The dependence on the opposition is strange and doesn't result from saturation of the HEMT. We believe the measurements with optimized opposition are more reliable.



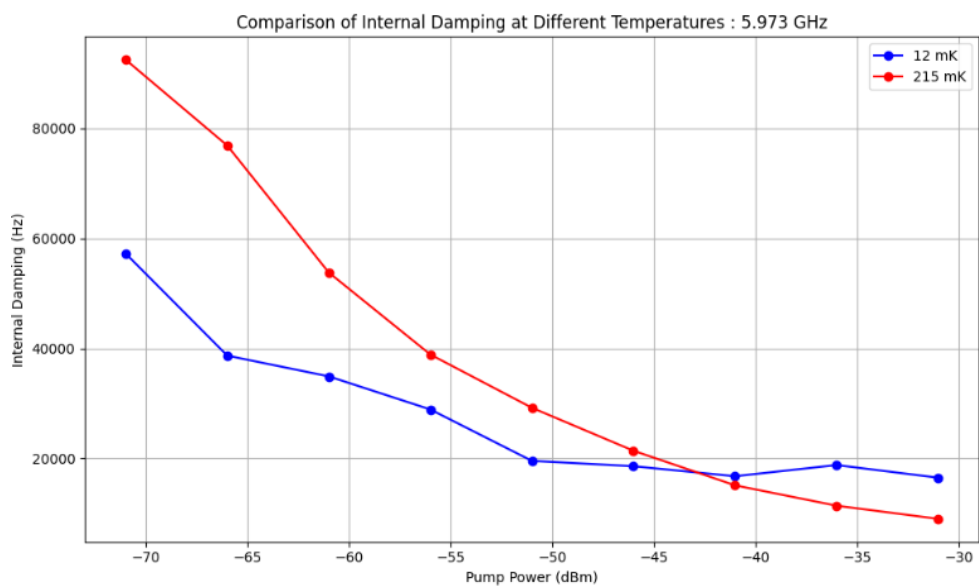
A small asymmetry parameter was necessary for a good fit:



Here is the temperature dependence of the pump power dependence of the internal damping. We believe that, at high pump powers, the measurements with opposition are more reliable than the ones without opposition. Has this temperature dependence been previously reported in microwave cavities?



Here is the T dependence of the 6.0 GHz mode.



3.2 Mechanics

We also measured the thermomechanical noise of the drum coupled to the 5.1 GHz cavity as a function of pump power. From p. 49 of my green notebook, according to the Fluctuation-Dissipation theorem, the position power spectral density of the thermomechanical noise in the limit $k_B T \gg \hbar \omega$ is

$$S_{xx} = \frac{2 \operatorname{Im}[\chi] k_B T}{\omega}$$

$$\operatorname{Im}[\chi] = \frac{\Gamma_m \omega}{m \left[(\Omega_m^2 - \omega^2)^2 + (\Gamma_m \omega)^2 \right]}$$

so

$$S_{xx} = \frac{2 \Gamma_m k_B T}{m \left[(\Omega_m^2 - \omega^2)^2 + (\Gamma_m \omega)^2 \right]}.$$

For $\omega \approx \Omega_m$,

$$\begin{aligned} S_{xx} &= \frac{k_B T}{m \Omega_m^2} \frac{2 \Gamma_m}{\left[4 (\omega - \Omega_m)^2 + \Gamma_m^2 \right]} \\ &= \frac{1}{2} \frac{k_B T}{m \Omega_m^2 \pi} \frac{\Gamma_m / 4\pi}{\left[(f - f_m)^2 + (\Gamma_m / 4\pi)^2 \right]} \end{aligned}$$

Since

$$\int_{-\infty}^{\infty} \frac{1}{\pi} \frac{c}{(x - x_0)^2 + c^2} dx = 1$$

we have

$$\int_0^{\infty} S_{xx} df = \frac{1}{2} \frac{k_B T}{m \Omega_m^2}$$

We can repeat the same approximation at $\omega \approx -\Omega_m$ to obtain $\langle x^2 \rangle = \int_{-\infty}^{\infty} S_{xx} df = k_B T / m \Omega_m^2$, in agreement with equipartition.

According to Eq. 2.92 of [6], the microwave output spectrum of the upper sideband of a green pump is, in units of photons,

$$\begin{aligned} S &= \frac{16 \Gamma_m \kappa_r g_0^2 n_d n_b}{4 (\omega - \Omega_m)^2 + \Gamma_m^2} \frac{1}{\kappa_{tot}^2 + 4 \Omega_m^2} \\ &= \frac{4 \kappa_r g_0^2 n_d n_b}{k_B T} \frac{m \Omega_m^2}{\kappa_{tot}^2 + 4 \Omega_m^2} S_x \\ &= \frac{4 \kappa_r g_0^2 n_d}{\hbar} \frac{m \Omega_m}{\kappa_{tot}^2 + 4 \Omega_m^2} S_x \\ &= \frac{2 \kappa_r G_{opto}^2 n_d}{\kappa_{tot}^2 + 4 \Omega_m^2} S_x \end{aligned}$$

where S_x is the single sided PSD and, from Eq. 2.67 of Sumit's thesis,

$$\begin{aligned} n_d &= \frac{4\kappa_l P_{in}}{\hbar\omega_d \left[\kappa_{tot}^2 + 4(\omega_c - \omega_d)^2 \right]} \\ &= \frac{4\kappa_l P_{RT} G_{atten}}{\hbar\omega_d \left[\kappa_{tot}^2 + 4(\omega_c - \omega_d)^2 \right]} \end{aligned}$$

where P_{RT} is the pump power at our room temperature reference point and G_{atten} is the attenuation between the reference point and the sample. We set $\kappa_l = \kappa_r = \Gamma_{ex}$ from the fits above.

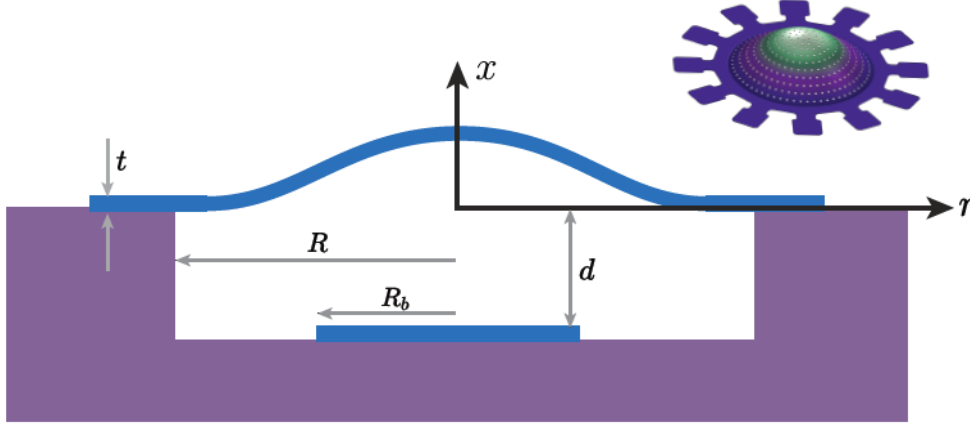
We used $d = 200$ nm, $t = 200$ nm, and $R = 100$ μ m. From Eq. 47 of [1], we used the effective mass

$$m = 0.27\rho\pi R^2 t$$

and from Eq. 54

$$g_0 = 0.37\sqrt{\hbar}\frac{\omega_c}{2d} (R^2 t^2 \rho \sigma_m)^{-1/4}$$

We assumed the stress in the Al $\sigma_m = 350$ MPa.

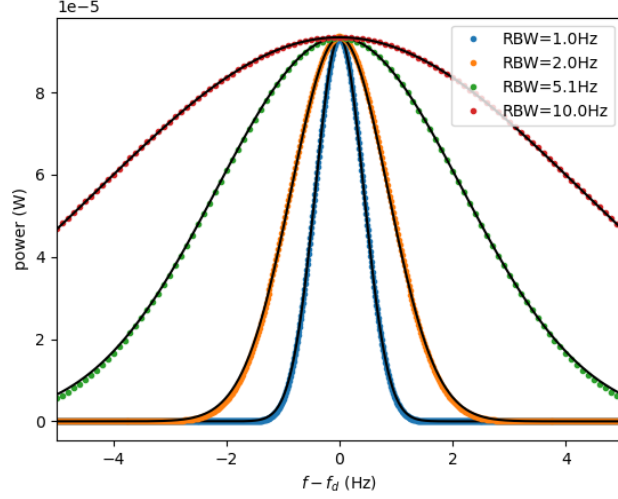


So the signal reaching the spectrum analyzer is, in units of W/Hz=Joules,

$$\begin{aligned} S_{RT} &= \hbar\omega_d G_{amps} S \\ &= \hbar\omega_d G_{amps} \frac{4\kappa_r g_0^2}{\hbar} n_d \frac{m\Omega_m}{\kappa_{tot}^2 + 4\Omega_m^2} S_x \end{aligned}$$

where G_{amps} is the gain of the amplifiers. In cavity sweeps we measured $S_{21} = -59$ dB away from the resonance and we had 66 dB of attenuation between the VNA output and our standard reference point. So $G_{atten} G_{amps} \equiv G$ and $10 \log G = 7$ dB.

$$S_{RT} = A S_x$$



where

$$\begin{aligned}
A &\equiv \hbar\omega_d G_{amps} \frac{4\kappa_r g_0^2}{\hbar} n_d \frac{m\Omega_m}{\kappa_{tot}^2 + 4\Omega_m^2} \\
&= P_{RT} G_{atten} G_{amps} \frac{4\kappa_r g_0^2}{\hbar} \frac{n_d \hbar\omega_d}{P_{RT} G_{atten}} \frac{m\Omega_m}{\kappa_{tot}^2 + 4\Omega_m^2} \\
&= P_{RT} G \frac{4\kappa_r g_0^2}{\hbar} \frac{m\Omega_m}{\kappa_{tot}^2 + 4\Omega_m^2} \frac{4\kappa_l}{\left[\kappa_{tot}^2 + 4(\omega_c - \omega_d)^2\right]}
\end{aligned}$$

According to the automatic output in the data file saved by the spectrum analyzer, it uses a Gaussian filter with a resolution bandwidth $RBW=1$ Hz. We tested this by connecting the Anapico directly to the spectrum analyzer and sending a signal with power P_{test} at a single frequency, ideally $S_{test}(f) = P_{test}\delta(f - f_d)$. We found that the analyzer convolves the input with $f_{fil} = \exp - \left(\frac{f}{\sqrt{2}\sigma_{RBW}}\right)^2$, so that the analyzer output in this test is given by

$$\begin{aligned}
S_{test} RBW &= P_{test} \int \delta(f' - f_d) \exp - \left(\frac{f - f'}{\sqrt{2}\sigma_{RBW}}\right)^2 df' \\
&= P_{test} \exp - \left(\frac{f - f_d}{\sqrt{2}\sigma_{RBW}}\right)^2
\end{aligned}$$

where $\sigma_{RBW} = \frac{RBW}{2\sqrt{2\ln 2}}$, and where the factor of RBW on the LHS accounts for the fact that the analyzer outputs the power in each frequency bin, not a spectral density. We get good agreement between theory and measurement:

The thermomechanical spectrum output by the analyzer is then

$$\begin{aligned}
S_{an}RBW &= S_{RT} \star f_{fil} \\
&= A \int S_x(f') \exp - \left(\frac{f - f'}{\sqrt{2}\sigma_{RBW}} \right)^2 df' \\
&= A \int \frac{4\Gamma_m k_B T}{m\Omega_m^2 \left[4(2\pi f' - \Omega_m)^2 + \Gamma_m^2 \right]} \exp - \left(\frac{f - f'}{\sqrt{2}\sigma_{RBW}} \right)^2 df' \\
&= A \frac{k_B T}{m\Omega_m^2} \int \frac{\Gamma_m / (4\pi)}{\pi \left[(f' - \Omega_m / (2\pi))^2 + (\Gamma_m / (4\pi))^2 \right]} \exp - \left(\frac{f - f'}{\sqrt{2}\sigma_{RBW}} \right)^2 df' \\
&= A \frac{k_B T}{m\Omega_m^2} \int \frac{\Gamma_m / (4\pi)}{\pi \left[(\Gamma_m / (4\pi))^2 + (f - \Omega_m / (2\pi) - f')^2 \right]} \exp - \left(\frac{f'}{\sqrt{2}\sigma_{RBW}} \right)^2 df'
\end{aligned}$$

According to https://en.wikipedia.org/wiki/Voigt_profile referenced by https://docs.scipy.org/doc/scipy/reference/generated/scipy.special.vogt_profile.html,

$$V(x; \sigma, \gamma) = \int_{-\infty}^{\infty} \frac{\gamma}{\pi \left[\gamma^2 + (x - x')^2 \right]} \frac{1}{\sqrt{2\pi}\sigma} \exp - \left(\frac{x'}{\sqrt{2}\sigma} \right)^2 dx'$$

and

$$\int_{-\infty}^{\infty} V(x; \sigma, \gamma) dx = 1$$

Identifying $\gamma = \Gamma_m / (4\pi)$, $x = f - \Omega_m / (2\pi)$, $x' = f'$, and $\sigma = \sigma_{RBW}$, we have

$$S_{an}RBW = A\sqrt{2\pi} \frac{k_B T}{m\Omega_m^2} \sigma_{RBW} V[f - \Omega_m / (2\pi); \sigma_{RBW}, \Gamma_m / (4\pi)]$$

and

$$\int_{-\infty}^{\infty} S_{an}RBW df = A\sqrt{2\pi} \frac{k_B T}{m\Omega_m^2} \sigma_{RBW}$$

We can fit $p_0 V[f - f_0; \sigma_{RBW}, \Delta f / 2] + p_3$ to the analyzer output and compare with the theoretical expression (see 'EPFL sample 1 5.089 GHz.ipynb').

Anushka subtracted $G_{amps} = 75$ dB from the analyzer output and fit $p_0 V[f - f_0; \sigma_{RBW}, \Delta f / 2] + p_3$ to the result. She obtained best fit values in agreement with mine, except for the offset, which differed by a factor of 2, but this doesn't enter into the comparison with theory. She then calculated $\frac{\pi}{2} p_0 \Delta f / \text{factor}$ where

$$\text{factor} = 2 \frac{\kappa_{ext} G^2 n_d \hbar \omega_d}{4\omega_m^2 + \kappa_{tot}^2}$$

and expected it to equal $\frac{k_B T}{m\Omega_m^2}$ (see 'sample 1 S21 and thermomechanics in transmission May 2025(UPDATED).ipynb'). So factor should equal my expression for $\frac{S}{S_x}$ derived above:

$$\frac{S}{S_x} = \frac{2\kappa_r G_{opto}^2 n_d}{\kappa_{tot}^2 + 4\Omega_m^2}$$

4 Fits of S11 measurements

Anushka fitted

$$S_{11} = \frac{\kappa_{ex} - \kappa_{in} + 2i\Delta\omega}{\kappa_{ex} + \kappa_{in} - 2i\Delta\omega}$$

to measurements at 100 mK of Sample 5.668 GHz device with an open termination of the sample box. See 'EPFL sample B 5.668 GHz 97 mK reflection.ipynb'.

References

- [1] A. Youssefi, S. Kono, M. Chegnizadeh, T. J. Kippenberg, *Nature Physics* **19**, 1697 (2023).
- [2] A. Youssefi, M. Chegnizadeh, M. Scigliuzzo, T. J. Kippenberg, *arXiv preprint arXiv:2501.03211* (2025).
- [3] K. Geerlings, *et al.*, *Applied Physics Letters* **100** (2012).
- [4] T. Capelle, *et al.*, *Physical Review Applied* **13**, 034022 (2020).
- [5] M. Von Schickfus, S. Hunklinger, *Physics Letters A* **64**, 144 (1977).
- [6] S. Kumar, Low temperature microwave optomechanics: anomalous force noise and optomechanically induced transparency, Ph.D. thesis, Univ. Grenoble Alpes (2021). <https://theses.hal.science/tel-03465023>.
- [7] M. Chegnizadeh, *et al.*, *Science* **386**, 1383 (2024).